Materials Research Express

PAPER

Information theoretic analysis of Landau levels in monolayer phosphorene under magnetic and electric fields

Materials Research Express

PAPER

Information theoretic analysis of Landau levels in monolayer phosphorene under magnetic and electric fields

Octavio Castaños[1], **Elvira Romera**[2] **and Manuel Calixto**[3,4]

[1] Instituto de Ciencias Nucleares, Universidad Nacional Autónoma de México, Apdo. Postal 70-543, 04510, CDMX, Mexico
[2] Departamento de Física Atómica, Molecular y Nuclear and Instituto Carlos I de Física Teórica y Computacional, Universidad de Granada, Fuentenueva s/n, 18071 Granada, Spain
[3] Departamento de Matemática Aplicada and Instituto Carlos I de Física Teórica y Computacional, Facultad de Ciencias, Universidad de Granada, Fuentenueva s/n, 18071 Granada, Spain
[4] Author to whom any correspondence should be addressed.

E-mail: ocasta@nucleares.unam.mx, eromera@ugr.es **and** calixto@ugr.es

RECEIVED
4 July 2019

REVISED
21 August 2019

ACCEPTED FOR PUBLICATION
30 August 2019

PUBLISHED
11 September 2019

Keywords: Phosphorene, edge states, tunable band gap, topological phase transition, information measures

Abstract

We analyze the structure of phosphorene Landau energy levels under electric and magnetic fields perpendicular to the material sheet. The electric field Δ provides a tunable band gap, and a topological phase transition occurs at a critical value Δ_c. Low energy Landau levels and edge states are analyzed with different information theoretic measures (like participation ratio, fidelity and entropy) and some order parameters, which turn out to be good markers of the topological phase transition.

1. Introduction

Phosphorene is a monolayer of black phosphorus, belonging to the group of 2D gapped Dirac materials similar to graphene, which has been studied theoretically and experimentally (it has been firstly synthesized by Bridgman [1–9]). In phosphorene there are sp^3 bonds with two different bond angles (96.34° and 103.09°), each atom has two neighbors at 2.224 Å and a third one at 2.44 Å and, due to these characteristics, it has an orthorhombic structure with a great stability. This anisotropic structure results in a lighter effective mass along the x axis (chair direction) and a heavier effective mass along the y axis (zig-zag direction). Phosporene is relevant for optical properties and it can be used as a photodetecting material [10]. It also has interest in the framework of field effect transistor applications in nanoelectronics [11–13], because of its direct band gap (up to 2eV) and a high carrier mobility (1000 $cm^2\,V^{-1}\,s^{-1}$) at room temperature. Phosphorene's electronic devices have been manufactured with considerable success, showing a great performance [7, 14–16].

The low energy physics of phosphorene can be described using an effective $\mathbf{k}\cdot\mathbf{p}$ Hamiltonian. The Landau levels (LLs) spectra and the magneto-transport properties of monolayer phosphorene under a perpendicular magnetic field have been investigated by Zhou *et al* [17]. The effect of a vertical electric field on the electronic band structure and transport of multilayer phosphorene has also been studied in [18]. In [19] and [20], a study of the even–odd and the giant Stark effects in zigzag and armchair edge states, respectively, for phosphorene nanoribbons under a transverse electric field, has been carried out. However, the effect of the electric field on LLs, as a trademark of the topological phase transition, has not been fully understood in phosphorene.

The application of a perpendicular electric field to the material sheet, in some 2D gapped materials analogous to graphene (such as silicene, germanene, stannene, etc.), provides a tunable band gap, and a topological phase transition occurs, from a topological insulator (TI) to a band insulator (BI), at a charge neutrality (gap cancellation) point [21]. In general a TI-BI transition is characterized by a band inversion with a level crossing at some critical value of a control parameter. Topological phases can be characterized by topological charges like Chern numbers [22]. Recently, information theoretic measures have been proved to be useful in the description and characterization of topological phase transitions [23–28].

In this paper we further explore the effects of electric and magnetic fields in the band structure of phosphorene, showing that there appears a topological phase transition at a critical value of this electric field.

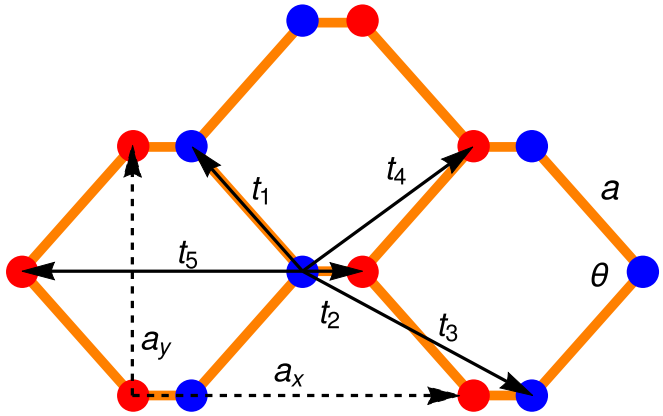

Figure 1. Top view of phosphorene. Red (blue) balls represent phosphorus atoms in the lower (upper) layer. The in-plane bond length and angle are $a = 2.22$ Åand $\theta = 96.79°$, respectively. The primitive vectors $a_x = 3.32$ Å and $a_y = 4.38$ Å are denoted by dashed arrows. The first five neighbor hopping sites t_j necessary to describe phosporene [29] are denoted by solid arrows.

The work is organized as follows. Firstly in section 2 we introduce the low energy Hamiltonian describing the properties of phosphorene in the presence of electric and magnetic fields. In section 3 we solve the eigenvalue problem for this Hamiltonian, studying the LLs and edge states. In section 4 we use information measures to describe the topological phase transition. Finally, section 5 is devoted to final conclusions.

2. Tight binding and low energy $k \cdot p$ model Hamiltonian

A tight binding model, $\tilde{H}_4 = \sum_{\langle i,j\rangle} t_{ij} c_i^\dagger c_j$, of phosphorene has been proposed by [29], where summation runs over lattice sites, t_{ij} is the transfer energy between sites i and j (it has been shown [29] that it is enough to consider five hopping links $t_1, ..., t_5$), and $c_i^\dagger$ (c_i) is the creation (annihilation) operator of electrons at site i. The unit cell of phosphorene contains four phosphorus atoms: two in the upper layer and two in the lower layer (see figure 1). Therefore, in the momentum representation, the energy dispersion of phosphorene is described by a four-band Hamiltonian $\tilde{H}_4 = \sum_{\mathbf{k}} c^\dagger(\mathbf{k}) H_4(\mathbf{k}) c(\mathbf{k})$ where (see [30])

$$H_4 = \begin{pmatrix} 0 & f_1 + f_3 & f_4 & f_2 + f_5 \\ \bar{f}_1 + \bar{f}_3 & 0 & f_2 & f_4 \\ \bar{f}_4 & \bar{f}_2 & 0 & f_1 + f_3 \\ \bar{f}_2 + \bar{f}_5 & \bar{f}_4 & \bar{f}_1 + \bar{f}_3 & 0 \end{pmatrix} \tag{1}$$

with

$$\begin{aligned} f_1 &= 2t_1 e^{\frac{ia_x k_x}{2\sqrt{3}}} \cos\left(\frac{a_y k_y}{2}\right), \quad f_2 = t_2 e^{-\frac{ia_x k_x}{\sqrt{3}}} \\ f_3 &= 2t_3 e^{\frac{5ia_x k_x}{2\sqrt{3}}} \cos\left(\frac{a_y k_y}{2}\right), \\ f_4 &= 4t_4 \cos\left(\frac{\sqrt{3}}{2} a_x k_x\right) \cos\left(\frac{a_y k_y}{2}\right), \quad f_5 = t_5 e^{\frac{2ia_x k_x}{\sqrt{3}}}, \end{aligned} \tag{2}$$

$\bar{f}_i$ is the conjugate of f_i, and (a_x, a_y) are the primitive vectors.

The four-band model can be reduced to a two-band model, due to the D_{2h} point group invariance (i.e., to consider two points, intead of four, per unit cell), with Hamiltonian

$$H_2 = \begin{pmatrix} f_4 & f_1 + f_2 + f_3 + f_5 \\ \bar{f}_1 + \bar{f}_2 + \bar{f}_3 + \bar{f}_5 & f_4 \end{pmatrix}, \tag{3}$$

with energy spectrum $E_\pm(\mathbf{k}) = f_4 \pm |f_1 + f_2 + f_3 + f_5|$ (strongly anisotropic) and band gap $E_g = 4t_1 + 2t_2 + 4t_3 + 2t_5$. Expanding around the Γ point of the Brillouin zone (up to second order in $\mathbf{k}$) and doing a coordinate rotation (for convenience, like in [17, 29]) of the Pauli matrices ($\sigma_x \to \sigma_z$, $\sigma_y \to \sigma_x$), one obtains the following simplified $\mathbf{k} \cdot \mathbf{p}$ model for phosphorene (we use the same notation as in [17])

$$H_2 = \begin{pmatrix} E_c + \alpha_x k_x^2 + \alpha_y k_y^2 & \gamma k_x \\ \gamma k_x & E_v + \beta_x k_x^2 + \beta_y k_y^2 \end{pmatrix}. \tag{4}$$

This will be our starting point. The hopping parameters are $t_1 = -1.220$ eV, $t_2 = 3.665$ eV, $t_3 = -0.205$ eV, $t_4 = -0.105$ eV, $t_5 = -0.055$ eV, and the lengths of the unit cell are $a_x = 3.32$ Å and $a_y = 4.38$ Å. With these values, the conduction and valence energies are $E_c = 0.34$ eV and $E_v = -1.18$eV, respectively, so that the energy gap is $E_g = E_c - E_v = 1.52$ eV. The off diagonal parameter $\gamma = -5.2305$eVÅ describes the interband coupling between the conduction and valence bands. As in Reference [17], it will be useful to relate the Hamiltonian parameters $\alpha_{x,y}$ and $\beta_{x,y}$ to some effective masses as $\alpha_{x,y} = \hbar^2/(2m_{cx,cy})$ and $\beta_{x,y} = \hbar^2/(2m_{vx,vy})$. For phosphorene, we have $m_{cx} = 0.793m_e$, $m_{cy} = 0.848m_e$, $m_{vx} = 1.363m_e$ and $m_{vy} = 1.142m_e$, where m_e denotes the free electron mass.

A perpendicular magnetic field $\mathbf{B} = (0, 0, B)$ can be introduced through the minimal (Peierls) substitution $\hat{\mathbf{p}} \to \hat{\mathbf{p}} - e\mathbf{A}$. Taking the Landau gauge $\mathbf{A} = (-By,\ 0,\ 0)$ and defining the the annihilation (and creation $\hat{a}^\dagger$) operator,

$$\hat{a} = \sqrt{\frac{m_{cy}\omega_c}{2\hbar}}\left(y - y_0 + i\frac{\hat{p}_y}{m_{cy}\omega_c}\right), \tag{5}$$

with $\omega_c = eB/\sqrt{m_{cx}m_{cy}}$, $y_0 = \ell_B^2 k_x$ and $\ell_B = \sqrt{\hbar/(eB)}$ the cyclotron frequency, center and magnetic length, respectively, the corresponding Hamiltonian adopts the following form

$$\begin{aligned} \hat{H}_2^B = {} & \hbar\omega_\gamma(\hat{a} + \hat{a}^\dagger)\sigma_x + \frac{E_c + \hbar\omega_c(\hat{a}^\dagger\hat{a} + 1/2)}{2}(\sigma_0 + \sigma_z) \\ & + \frac{E_v - \hbar\omega_v(\hat{a}^\dagger\hat{a} + 1/2) - (\hat{a}^2 + \hat{a}^{\dagger 2})\hbar\omega'}{2}(\sigma_0 - \sigma_z), \end{aligned} \tag{6}$$

where $\omega_\gamma = \gamma/\sqrt{2}\,\hbar\ell_B\rho$, $\omega_v = (r_x + r_y)\omega_c$ and $\omega' = (r_x - r_y)\omega_c/2$, with $\rho = (m_{cy}/m_{cx})^{1/4}$, $r_{x,y} = m_{cx,cy}/(2m_{vx,vy})$ and σ_0 is the two-dimensional identity matrix.

In addition to the magnetic field, we shall add an electric field interaction in the usual form $\hat{H}_2^\Delta = \Delta\sigma_z$, with Δ the electric potential. Therefore, our total Hamiltonian will be

$$\hat{H}_2 = \hat{H}_2^B + \hat{H}_2^\Delta. \tag{7}$$

The role of the electric field will be to provide a tunable band gap.

3. Diagonalization: parity, Landau levels and edge states

Let us denote by $|n,\ s\rangle$ the basis states of our Hilbert space, with $n = 0,1,2,\ldots$, the eigenvalues of $\hat{n} = \hat{a}^\dagger\hat{a}$ and $s = \pm 1$ the eigenvalues of σ_z. For convenience, in the following analysis, we are disregarding the degeneracy in k_x due to translational invariance in the x axis. Firstly we notice that time evolution with $\hat{H}_2$ preserves the parity $\pi(n,\ s) = e^{i\pi n_s}$ of the state $|n,\ s\rangle$, with $n_s = n + (s+1)/2$. That is, the parity operator $\hat{\Pi} = e^{i\pi\hat{n}_\sigma}$, with $\hat{n}_\sigma = \hat{n} + (\sigma_z + \sigma_0)/2$, commutes with $\hat{H}_2$. Therefore, both operators can then be jointly diagonalized. This means that the matrix elements $\langle n,\ s|\hat{H}_2|n',\ s'\rangle \propto \delta_{\pi(n,s),\pi(n',s')}$ are zero between states of different parity. This parity symmetry helps in the diagonalization process. Indeed, any (non-degenerate) eigenstate of $\hat{H}_2$ has a definite parity. We shall denote by

$$|\psi_k\rangle = \sum_{n,s} c_{n,s}^{(k)}|n,\ s\rangle \tag{8}$$

the Hamiltonian eigenstates with LL index $k \in \mathbb{Z}$ ($k > 0$ for conduction and $k < 0$ for valence band). The sum $\sum_{n,s}$ is constrained to $\pi(n,s) = \pm 1$, depending on the even (+) and odd (−) parity of k. The coefficients $c_{n,s}^{(k)}$ are obtained by numerical diagonalization of the Hamiltonian matrix, which is truncated to $n \leqslant N$, with N large enough to achieve convergent results for given values of the magnetic and electric fields. In order to study the effect of a band inversion (topological phase transition), we shall consider electric potentials around $\Delta \simeq -E_g = -1.52$ eV, more precisely, we shall analyze the window $-2.2 \leqslant \Delta \leqslant -1.0$. For a magnetic field of $B = 10$ T (like the one used in [17]), convergence is achieved for $N = 450$ states, with an error in the energies less than 10^{-9}, inside the range $-2.2 \leqslant \Delta \leqslant -1.0$. We have seen that N must grow with $|\Delta|$ for $\Delta < -2.2$ (topological insulator region) in order to achieve convergence. Similar qualitative results are obtained for lower values of the magnetic field.

In figure 2 we represent the electronic band structure of phosphorene as a function of the electric potential Δ. We select the first 13 low energy LLs $k = -6,\ldots,0,\ldots,6$: 6 valence states (3 even plus 3 odd), 6 conduction states (3 even plus 3 odd) and the edge state $k = 0$ (black solid line). Even conduction states are in blue and even valence states in red. Odd states (both valence and conduction) are in dashed black. The edge state $k = 0$

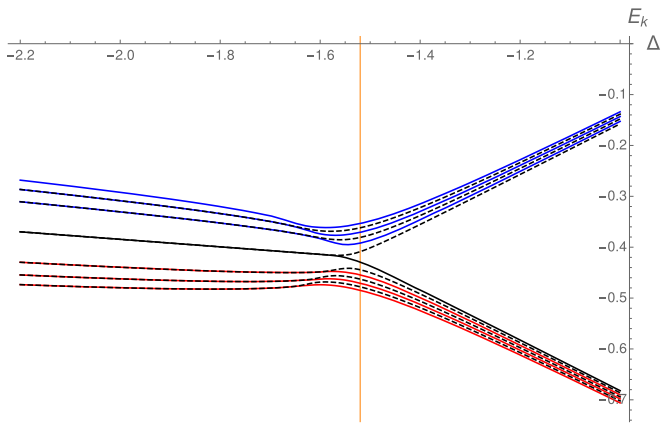

Figure 2. Low energy spectra E_k of phosphorene as function of the electric field strength Δ for thirteen LLs $k = -6,\ldots,0,\ldots,6$ (magnetic field $B = 10$ T). Valence (conduction) band LLs of even parity $k = -6, -4, -2$ ($k = 6, 4, 2$) are represented in red (blue) color. Odd parity LLs $k = \pm 5, \pm 3, \pm 1$ are represented by black dashed lines. The edge state $k = 0$ (with even parity) in solid black suffers band inversion around $\Delta_c = -1.52$ eV (marked with a vertical orange gridline) and degenerates with the odd parity conduction band LL $k = 1$ for $\Delta < \Delta_c$. Note that this degeneracy extends to other (even and odd) states at some values $\Delta < \Delta_c$ of the electric field. These values agree with the minima values of the fidelity in figure 6.

undergoes a band inversion around the critical value $\Delta_c = -E_g$, thus indicating the presencce of a topological phase transition from a band insulator to a topological insulator phase. Note that even and odd parity eigenstates degenerate for $\Delta < \Delta_c$ (topological insulator regime) inside the conduction and valence bands. The edge state $k = 0$ and the first conduction LL $k = 1$ (odd) degenerate for $\Delta < \Delta_c$.

Let us have a closer look to the structure of these first 13 low energy LLs. Actually, we shall restrict ourselves to the even parity conduction (blue) and valence (red) eigenstates, together with the edge state (solid black), since odd states display a similar behavior. To analyze the structure of these LLs, we shall use different information theoretic measures and order parameters, which turn out to be good markers of the topological phase transition.

4. Information measures of energy eigenstates and topological phase transition

We shall start by studying the expectation value $\langle \hat{n} \rangle$ of the number operator $\hat{n}$, its standard deviation Δn, together with the occupation probability $\langle \sigma_z \rangle$ of the valence and conduction bands. We shall see that they turn out to be good markers of the topological phase transition occurring at $\Delta_c = -E_g = -1.52$ eV, from the band insulator region $\Delta > \Delta_c$ to the topological insulator regime $\Delta < \Delta_c$.

The calculation of these quantities is done by determining the corresponding reduced density matrix of the Hamiltonian eigenstate (8) in the Landau (L) and band (B) sectors. More precisely, tracing out the band (conduction $s = 1$ and valence $s = -1$) indices from the density matrix $\rho_k = |\psi_k\rangle \langle \psi_k|$, we arrive to the reduced density matrix in the Landau sector

$$\rho_k^L = \sum_{s,n,n'} c_{n,s}^{(k)} \, \bar{c}_{n',s}^{(k)} |n\rangle \langle n'|. \tag{9}$$

In the same manner, tracing out the LL indices from ρ_k, we arrive to the reduced density matrix in the band sector

$$\rho_k^B = \sum_{n,s,s'} c_{n,s}^{(k)} \, \bar{c}_{n,s'}^{(k)} |s\rangle \langle s'|. \tag{10}$$

Therefore one has,

$$\begin{aligned} \langle \hat{n} \rangle_k &= \mathrm{tr}(\rho_k^L \, \hat{n}\,) = \sum_n n \, \mathcal{P}_k(n), \\ (\Delta n)_k &= \sqrt{\langle \hat{n}^2 \rangle_k - \langle \hat{n} \rangle_k^2}\,, \\ \langle \sigma_z \rangle_k &= \mathrm{tr}(\rho_k^B \, \sigma_z\,) = \sum_s s \, \mathcal{P}_k(s), \end{aligned} \tag{11}$$

where we have defined the probability of the eigenstate $|\psi_k\rangle$ to be at the Landau level n as $\mathcal{P}_k(n) = \sum_s |c_{n,s}^{(k)}|^2$, and the probability to be at the band s as $\mathcal{P}_k(s) = \sum_n |c_{n,s}^{(k)}|^2$. The results are shown in figures 3 and 4, where we represent the expectation values of $\hat{n}$ and σ_z as function of the electric potential strength Δ for the first six even low energy LLs $k = \pm 6, \pm 4, \pm 2$ and the edge state $k = 0$.

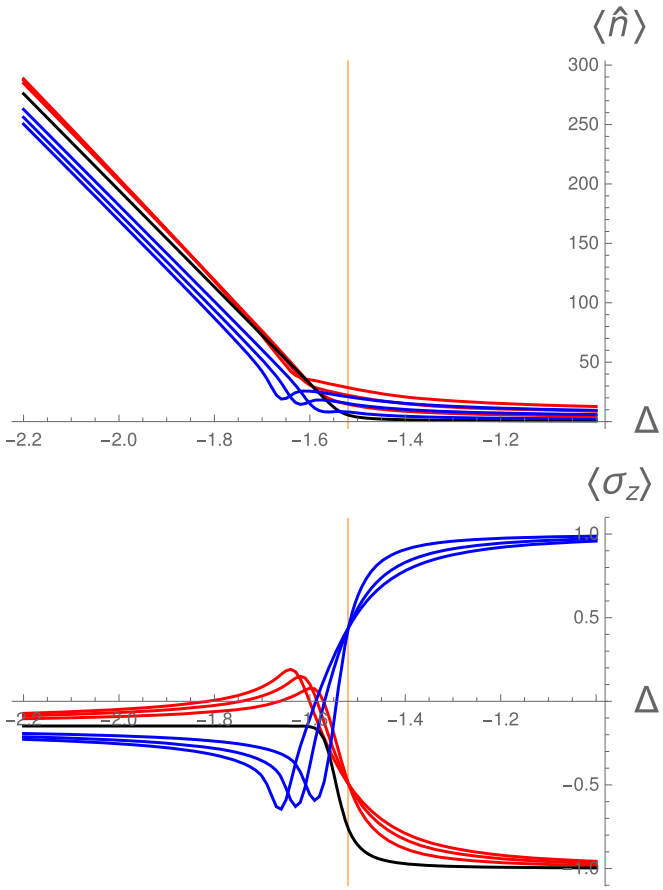

Figure 3. Expectation values of $\hat{n}$ and σ_z as function of the electric potential strength Δ for the first six even low energy LLs $k = \pm 6$, ± 4, ± 2 and the edge state $k = 0$ (in black); conduction band LLs in blue and valence band LLs in red. The critical point $\Delta_c = -1.52$ eV, separating the band from the topological insulator regime, is marked with a vertical orange grid line.

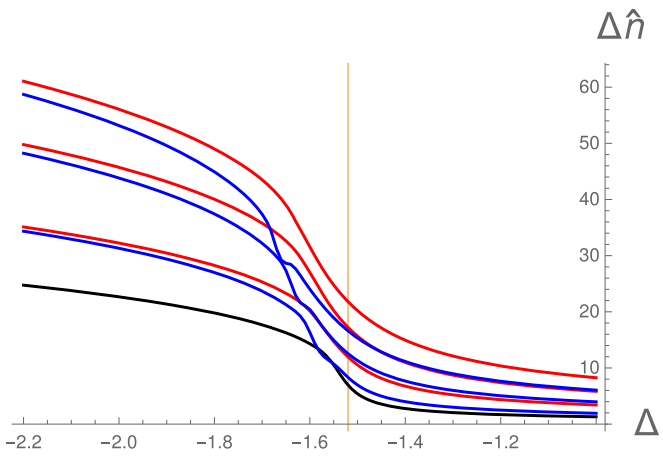

Figure 4. Standard deviation $\Delta\hat{n}$ as function of the electric potential strength Δ for the first six even low energy LLs and the edge state (in black); conduction band LLs in blue and valence band LLs in red. The critical point $\Delta_c = -1.52$ eV is marked with a vertical orange grid line.

We appreciate that both, conduction and valence low energy LLs, have a small expectation value $\langle \hat{n} \rangle$ in the band insulator region and a high one (smaller than the threshold $N = 450$ used to achieve convergence) in the topological insulator regime. The standard deviation $\Delta\hat{n}$ in figure 4 has a similar behavior. This means that the low energy LLs participate of more and more basis states $|n, s\rangle$, with higher and higher n, as we move from the band to the topological insulator regions, with a sudden change at the critical point Δ_c. This can be better appreciated by computing the inverse participation ratio (IPR) of a given LL (8), which is defined as:

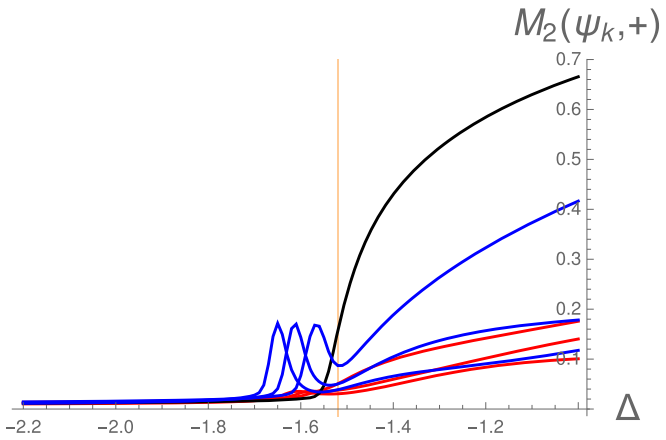

Figure 5. Inverse participation ratio of the first 7 low energy even LL (3 conduction band states in blue, 3 valence band states in red and edge state in black) as a function of the electric potential. The critical point $\Delta_c = -1.52$ eV is marked with a vertical orange grid line.

$$M_2(\psi_k) = \sum_{n,s}^{N} |c_{n,s}^{(k)}|^4. \tag{12}$$

The IPR is $M_2(\psi) = 1$ when ψ participates on only one single state $|n,\ s\rangle$, whereas it is $M_2(\psi) = 1/N \to 0$ when ψ participates of all basis states with the same probability $|c_{n,s}^{(k)}|^2 = 1/N$; this is why it is denominated 'inverse' participation ratio. In figure 5 we represent the IPR for the low energy LLs.

In figure 4 we also represent the expectation value $\langle\sigma_z\rangle$, which gives information about which kind of basis states $|n,\ s\rangle$ (conduction $s = 1$ or valence $s = -1$) participate on a given LL. We observe that, in the band insulator regime, conduction LLs mainly participate of states $|n,\ s\rangle$ with $s = 1$ (that is, $\langle\sigma_z\rangle \simeq 1$), whereas valence LLs mainly participate of states $|n,\ s\rangle$ with $s = -1$ (that is, $\langle\sigma_z\rangle \simeq -1$), as expected. However, as we move to the topological insulator region, both conduction and valence LLs equally participate of states $|n,\ s\rangle$ with $s = \pm 1$ (that is, $\langle\sigma_z\rangle \simeq 0$). Again, there is a sudden change of behavior for $\langle\sigma_z\rangle$ as we cross the critical point Δ_c.

This sudden change of behavior in the internal structure of LLs, when crossing the critical point, is better appreciated with another interesting information-theoretic concept like 'fidelity', widely used as, for example, a precursor of a quantum phase transsition. Fidelity is defined by

$$F_\psi(\Delta,\ \delta\Delta) = |\langle\psi(\Delta)|\psi(\Delta + \delta\Delta)\rangle|^2. \tag{13}$$

It is a measure of the distance between two close states $\psi(\Delta)$ and $\psi(\Delta + \delta\Delta)$, with $\delta\Delta \ll 1$. Therefore, it has values in the range $0 \leqslant F \leqslant 1$, with $F = 1$ indicating that the states are the same (up to a global phase) and $F = 0$ when they are orthogonal. In figure 6 we plot the fidelity for the low energy LLs (valence, conduction and edge), using $\delta\Delta = 0.025$. We see that LLs suffer a drastic structural change, with a sudden descent of the fidelity F, around the critical point Δ_c.

For completeness, we have also studied quantum correlations between level n and band s spaces for low energy even parity LLs as a function of Δ (the odd parity case yields similar results). To measure correlations, we have used the linear entropy $S_L(k) = 1 - \mathrm{tr}(\varrho_k^2)$, where ϱ_k is either the reduced density matrix in the Landau sector (9) or in the band sector (10). The explicit expression of the linear entropy can be given trough the purity

$$\mathrm{tr}(\varrho_k^2) = \sum_{n,n',s,s'} c_{n,s}^{(k)} c_{n,s'}^{(k)} \bar{c}_{n',s}^{(k)} \bar{c}_{n',s'}^{(k)}. \tag{14}$$

The results are included in figure 7. The linear entropy ranges from $S_L = 0$ (no correlations) in the band insulator regime $\Delta \gg \Delta_c$ to $S_L = 1/2$ (maximally entangled) in the topological insulator regime $\Delta \ll \Delta_c$. This behavior is common to valence, conduction and edge states. The value $S_L = 1/2$ typically corresponds to a parity symmetric state, which has an even and odd contribution of equal weight.

5. Conclusions

We have seen that a topological-band insulator transition can be induced in phosphorene through an external electric field, which provides a tunable band gap. We have studied several properties of low energy Landau levels, as a function of the electric field, in the topological and band insulator regimes, which provide good signatures and markers of the corresponding transition. We have computed the low energy spectra (by numerical diagonalization of the Hamiltonian) and showed the existence of edge states suffering a band inversion. Level $\langle\hat{n}\rangle$

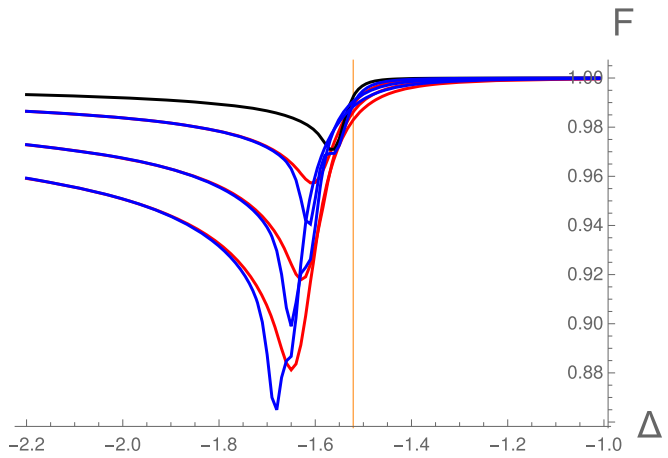

Figure 6. Fidelity as a function of the electric potential strength for the first seven $k = \pm 6, \pm 4, \pm 2, 0$ low energy, valence (red) conduction (blue) and edge (black), even LLs. The critical point is marked with a vertical orange grid line.

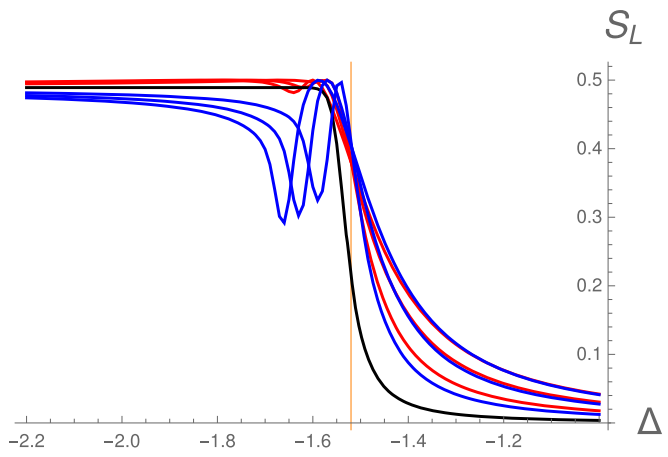

Figure 7. Linear entropy measuring level and band correlations as a function of the electric potential for the first seven $k = \pm 6, \pm 4, \pm 2, 0$ low energy, valence (red) conduction (blue) and edge (black), even LLs. The critical point is marked with a vertical orange grid line.

and band $\langle \sigma_z \rangle$ number expectation values display a sudden change of behavior across the critical point. This abrupt change in the low energy Landau levels is also captured by other information measures like: the inverse participation ratio M_2, fidelity F and linear entropy S_L, the last one evidencing the appearance quantum correlations between level n and band s quantum numbers in the topological insulator phase. These measures provide information about the different internal structure of Landau levels in the topological and band insulator regimes.

Electric-field modulation of phosphorene can realize, among other device functionalities, a field-effect transistor action. We believe that phosphorene can provide nano-electronic devices based on the emergence of new and exotic physical properties.

Acknowledgments

This study has been partially financed by the Consejería de Conocimiento, Investigación y Universidad, Junta de Andalucía and European Regional Development Fund (ERDF), under projects with Ref. SOMM17/6105/UGR and FQM381, and by the spanish MICINN under project PGC2018-097831-B-I00. O. C. thanks support of the project DGAPA:IN101619.

ORCID iDs

Octavio Castaños https://orcid.org/0000-0003-2514-3764
Manuel Calixto https://orcid.org/0000-0002-2566-9590

References

[1] Corbridge D 2013 *Phosphorus: Chemistry, Biochemistry and Technology* 6th edn (Boca Raton, FL: CRC Press)
[2] Bridgman P W 1914 Two new modifications of phosphorus *J. Am. Chem. Soc.* **36** 1344–63
[3] Bridgman P W 1916 Further note on black phosphorus *J. Am. Chem. Soc.* **38** 609–12
[4] Zhu Z and Tománek D 2014 Semiconducting layered blue phosphorus: a computational study *Phys. Rev. Lett.* **112** 176802
[5] Guo H, Lu N, Dai J, Wu X and Zeng X C 2014 Phosphorene nanoribbons, phosphorus nanotubes, and van der Waals multilayers *J. Phys. Chem.* C **118** 14051–9
[6] Guan J, Zhu Z and Tománek D 2014 Phase coexistence and metal-insulator transition in few-layer phosphorene: a computational study *Phys. Rev. Lett.* **113** 046804
[7] Li L *et al* 2014 Black phosphorus field-effect transistors *Nat. Nanotechnol.* **9** 372–7
[8] Rodin A S, Carvalho A and Castro Neto A H 2014 Strain- induced gap modification in black phosphorus *Phys. Rev. Lett.* **112** 176801
[9] Liu H *et al* 2014 Phosphorene: an unexplored 2D semiconductor with a high hole mobility *ACS Nano* **8** 4033–41
[10] Carvalho A, Wang M, Zhu X, Rodin A S, Su H and Castro-Neto A H 2016 Phosphorene: from theory to applications *Nature Review Materials* **1** 1–16
[11] Wan R, Cao X and Guo J 2014 Simulation of Schottky-barrier phosphorene transistors *Appl. Phys. Lett.* **105** 163511
[12] Liu H, Du Y, Deng Y and Ye P D 2015 Semiconducting black phosphorus: synthesis, transport properties and electronic applications *Chem. Soc. Rev.* **44** 2732
[13] Akhtar M, Anderson G, Zhao R, Alruqi A, Mroczkowska J E, Sumanasekera G and Jasinski J B 2017 Recent advances in synthesis, properties, and applications of phosphorene *NPJ 2D Mater. Appl.* **1** 5
[14] Chen P, Li N, Chen X, Ong W and Jand Zhao X 2017 The rising star of 2D black phosphorus beyond graphene: synthesis, properties and electronic applications *2D Mater* **5** 014002
[15] Ling X, Wang H, Huang S, Xia F and Dresselhaus M S 2015 The renaissance of black phosphorus *Proc. Natl Acad. Sci. USA* **112** 4523
[16] Xu R *et al* 2016 Extraordinarily bound quasi-one- dimensional trions in two-dimensional phosphorene atomic semiconductors *ACS Nano* **10** 2046
[17] Zhou X Y *et al* 2015 Landau levels and magneto-transport property of monolayer phosphorene *Sci. Rep.* **5** 12295
[18] Soleimanikahnoj S and Knezevic I 2017 Tunable electronic properties of multilayer phosphorene and its nanoribbons *J Comput Electron* **16** 568–75
[19] Zhou B, Zhou B, Zhou X and Zhou G 2017 Even-odd effect on the edge states for zigzag phosphorene nanoribbons under a perpendicular electric field *J. Phys. D: Appl. Phys.* **50** 045106
[20] Zhou B, Zhou B, Liu P and Zhou G 2018 The giant Stark effect in armchair-edge phosphorene nanoribbons under a transverse electric field *Phys. Lett.* A **382** 193
[21] Tahir M and Schwingenschlogl U 2013 Valley polarized quantum Hall effect and topological insulator phase transitions in silicene *Sci. Rep.* **3** 1075
[22] Ezawa M 2015 Monolayer topological insulators: silicene, germanene and stanene *J. Phys. Soc. Jap.* **84** 121003
[23] Calixto M and Romera E 2015 Identifying topological-band insulator transitions in silicene and other 2D gapped Dirac materials by means of Renyi-Wehrl entropy *Europhysics Letters.* **109** 40003
[24] Romera E and Calixto M 2015 Uncertainty relations and topological-band insulator transitions in 2D gapped Dirac materials *J. Phys. Condens. Matter* **27** 175003
[25] Bolívar J C, Nagy Á and Romera E 2018 Rényi-Fisher entropy product as a marker of topological phase transitions *Physica* A **498** 66
[26] Calixto M and Romera E 2015 Inverse participation ratio and localization in topological insulator phase transitions *Journal of Statistical Mechanics* P06029
[27] Bolívar J C, Romera E, Cordero N A and Nagy Á 2018 Fidelity as a marker of topological phase transitions in 2D Dirac materials *Int. J. Quantum Chem.* **118** e25674
[28] Romera E, Calixto M and Bolívar J C 2018 Information measures and topological-band insulatro transitions in 2D-Dirac materials under external circularly polarized lasers, and static electric and magnetic fields *Physica* A **511** 174
[29] Rudenko A N and Katsnelson M I 2014 Quasiparticle band structure and tight-binding model for single- and bilayer black phosphorus *Phys. Rev.* B **89** 201408(R)
[30] Ezawa M 2014 Topological origin of quasi-flat edge band in phosphorene *New J. Phys.* **16** 115004